Preprints of the 21st IFAC World Congress (Virtual)
Berlin, Germany, July 12-17, 2020

Lyapunov-based online Parameter Estimation for Continuous Fluidized Bed Layering Granulation

E. Otto * **C. Neugebauer** * **S. Palis** * **A. Kienle** *,**

* *Institute for Automation, Otto von Guericke University Magdeburg, Magdeburg, Germany (e-mail: eric.otto@ovgu.de).*
** *Max Planck Institute for Dynamics of Complex Technical Systems, Magdeburg, Germany*

Abstract: This paper is concerned with online parameter identification of milling behavior in fluidized bed layering granulation with external sieve-mill-cycle. A mill function is approximated with weighted Gaussian ansatz functions using a Lyapunov-based parameter estimation algorithm with a process model and plant data. The plant data is both generated by simulations and measured in experiments. In addition to previous work, the asymptotic convergence of the parameter estimator is proven theoretically. The identified mill function is validated by simulation of the process. It is shown that the plant and the identified model are in good agreement near the desired steady state.

Keywords: Particulate processes, parameter estimation, Lyapunov methods

1. INTRODUCTION

Fluidized bed layering granulation (FBLG) is a particle forming process with a wide range of applications in the pharmaceutical and food processing industry (Mörl et al., 2007). In order to produce particles with specified properties a suspension is sprayed on a particle bed fluidized with a heated stream of gas. After the evaporation of the liquid fraction the solid fraction remains on the particles resulting in layer wise growth.

In the continuous operation mode, which has various advantages such as higher production rates, particles are continuously removed from the bed. Therefore, new nuclei have to be supplied continuously, which is realized by grinding of oversized particles. The resulting process scheme is depicted in Fig. 1. Experimental investigations have shown self-sustained, non-linear oscillations in the particle size distribution (PSD) in continuous operation mode (Schmidt et al., 2015). These instabilities cause undesired variations in product properties or may even lead to a shut down of the process. The reasons leading to these instabilities were investigated in various model based studies (Radichkov et al., 2006; Dreyschultze et al., 2015). There it has been shown that operation parameters, in particular those regarding the milling process, are crucial for stability. In order to ensure a stable process operation, either the process conditions have to be chosen carefully or a stabilizing controller has to be applied. The latter has been investigated theoretically (Palis and Kienle, 2012, 2014) and experimentally (Neugebauer et al., 2019). The basis for the aforementioned control strategies has been a well-tuned process model including the milling process.

Few approaches in this direction have been made so far. Neugebauer et al. (Neugebauer et al., 2019) established

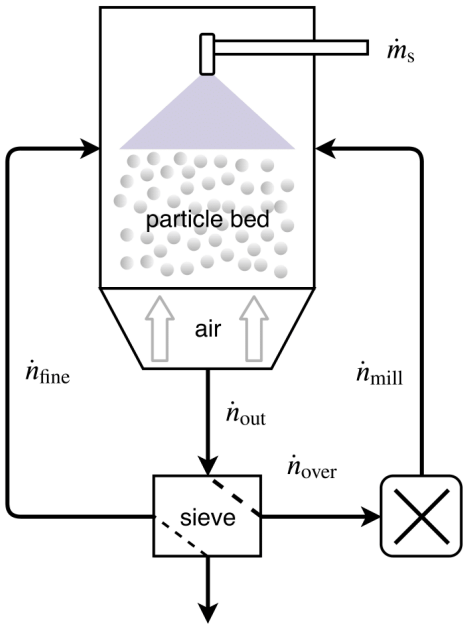

Fig. 1. Process scheme with granulation chamber, screening and mill

an empirical model of the grinding process based on preliminary offline experiments. A Lyapunov-based online estimation procedure using a low number of basis functions and simulation data has been proposed in Palis and Kienle (2017). In this contribution, a generalized version using a number of Gaussian basis functions will be investigated using experimental data from a measurement of the PSD.

The paper is structured as follows: In the second section a mathematical model of the process is presented. The

third section contains the derivation of the parameter estimator as well as its application to a simulated and an experimental case study. The results are summarized in section 4.

2. PROCESS MODELING

The fluidized bed layering granulation process can be modeled using population balance equations (PBEs). Here, the polydisperse particle population inside the granulation chamber is described in terms of the number density distribution $n(L,t)$, where the internal coordinate L represents the characteristic particle length and t is the time. The model used here is based on the equations derived in Heinrich et al. (2002). The following balance equation represents the dynamic behavior of the particle population

$$\frac{\partial n}{\partial t} = -G\frac{\partial n}{\partial L} + \dot{n}_{\text{in}} - \dot{n}_{\text{out}} \tag{1}$$

with growth rate G, particle inlet $\dot{n}_{\text{in}}$ and particle outlet $\dot{n}_{\text{out}}$.

It is assumed that the particles are non-porous spheres and that the particles and the injected suspension are distributed homogeneously in the granulation chamber. According to Mörl et al. (2007) the size-independent growth rate can be described as

$$G = \frac{2\dot{m}_{\text{inj}}}{\rho\pi\mu_2(n)} \tag{2}$$

with the injection rate of solid material $\dot{m}_{\text{inj}}$ and the second moment of the number density distribution

$$\mu_2(n) = \int_0^\infty L^2 n(L,t)\,\mathrm{d}L \tag{3}$$

which correlates to the total particle surface.

The particle outlet is assumed to be classified with classification function $T_{\text{out}}(L)$. The drain K determines the amount of discharged particles.

$$\dot{n}_{\text{out}}(L,t) = T_{\text{out}} K n \tag{4}$$

After the discharge the particle population is divided into an oversized fraction $\dot{n}_{\text{over}}$, a product fraction $\dot{n}_{\text{prod}}$ and fine population $\dot{n}_{\text{fine}}$ using two screens. The three fractions are given by

$$\begin{aligned} \dot{n}_{\text{over}}(L,t) &= T_{\text{sc1}}\dot{n}_{\text{out}} \\ \dot{n}_{\text{prod}}(L,t) &= T_{\text{sc2}}(1-T_{\text{sc1}})\dot{n}_{\text{out}} \\ \dot{n}_{\text{fine}}(L,t) &= (1-T_{\text{sc2}})(1-T_{\text{sc1}})\dot{n}_{\text{out}} \end{aligned} \tag{5}$$

with screening functions $T_{\text{sc1/sc2}}(L)$. The oversized particles are ground up and then fed back into the granulation chamber together with the fine fraction

$$\dot{n}_{\text{in}} = \dot{n}_{\text{mill}} + \dot{n}_{\text{fine}} \tag{6}$$

while the product fraction is removed from the process. Both the classification function T_{out} and the screen functions $T_{\text{sc1,sc2}}$ are given by cumulative Gaussian distributions

$$T_j(L) = \frac{\int_0^L \exp\left(\frac{-(L-L_j)^2}{2\sigma_j^2}\right)\mathrm{d}L}{\int_0^\infty \exp\left(\frac{-(L-L_j)^2}{2\sigma_j^2}\right)\mathrm{d}L} \tag{7}$$

with $j = \{\text{out}, \text{sc1}, \text{sc2}\}$ and the separation diameters L_j and variances σ_j Neugebauer et. al. (Neugebauer et al., 2019).

The milling can be modeled as a static process by

$$\dot{n}_{\text{mill}} = \varphi(L)\int_0^\infty L^3 \dot{n}_{\text{over}}\,\mathrm{d}L \tag{8}$$

with the normalized PSD of the milled particles $\varphi(L)$ and the total volume of oversized particles $\int_0^\infty L^3\dot{n}_{\text{over}}\,\mathrm{d}L$. Although experimental investigations (Neugebauer et al., 2016) suggest that $\dot{n}_{\text{mill}}$ can be described as the sum of three distributions, their specific shape is in general not known in advance and may vary during process operation. Therefore, the weighted sum of some Gaussian ansatz functions $\varphi_i(L)$ is used in this contribution.

$$\varphi(L) = \sum_{i=1}^{N} a_i \varphi_i(L) \tag{9}$$

Due to the mass-conservation of the milling processes, i.e.

$$\int_0^\infty L^3\dot{n}_{\text{over}}\,\mathrm{d}L = \int_0^\infty L^3\dot{n}_{\text{mill}}\,\mathrm{d}L \tag{10}$$

an additional constraint on the weights a_i results

$$\int_0^\infty L^3 \sum_{i=1}^{N} a_i\varphi_i(L)\,\mathrm{d}L = 1. \tag{11}$$

Solving this equation for the N-th parameter gives

$$a_N = \frac{1 - \int_0^\infty L^3 \sum_{i=1}^{N-1} a_i\varphi_i(L)\,\mathrm{d}L}{\int_0^\infty L^3\varphi_N(L)\,\mathrm{d}L} \tag{12}$$

which allows us to rewrite the mill fraction depending only on $N-1$ parameters as follows

$$\dot{n}_{\text{mill}} = \left(\sum_{i=1}^{N-1} a_i\phi_i(L) + \bar{\varphi}(L)\right)\int_0^\infty L^3\dot{n}_{\text{over}}\,\mathrm{d}L \tag{13}$$

with

$$\phi_i(L) = \varphi_i(L) - \frac{\int_0^\infty L^3\varphi_i(L)\,\mathrm{d}L}{\int_0^\infty L^3\varphi_N(L)\,\mathrm{d}L}\varphi_N(L) \tag{14}$$

and

$$\bar{\varphi}(L) = \frac{\varphi_N(L)}{\int_0^\infty L^3\varphi_N(L)\,\mathrm{d}L} \tag{15}$$

To ensure constant bed mass m_{bed}, which is crucial to a continuous operation of the process, the drain K is chosen such that $\dot{\mu}_3 = 0$ holds, where μ_3 corresponds to the total particle volume

$$\mu_3(n) = \int_0^\infty L^3 n(L,t)\,\mathrm{d}L\,. \tag{16}$$

The drain K is thus given by

$$K = \frac{\mu_3(-G\frac{\partial n}{\partial L})}{\mu_3\left(T_{\text{out}}T_{\text{sc2}}(1-T_{\text{sc1}})n\right)} \tag{17}$$

resulting in the following process model:

$$\begin{aligned} \frac{\partial n}{\partial t} =& -G\frac{\partial n}{\partial L} + \left(T_{\text{sc1}}T_{\text{sc2}} - T_{\text{sc2}} - T_{\text{sc1}}\right)T_{\text{out}}Kn \\ &+ \left(\sum_{i=1}^{N-1} a_i\phi_i(L) + \bar{\varphi}(L)\right)\int_0^\infty L^3\dot{n}_{\text{over}}\,\mathrm{d}L\,. \end{aligned} \tag{18}$$

3. LYAPUNOV-BASED PARAMETER IDENTIFICATION

As has been mentioned above, the shape of the particle size distribution resulting from the mill and thus appropriate weights a_i are in general unknown and may vary over time.

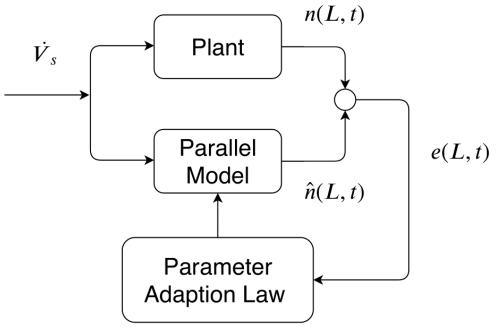

Fig. 2. Parameter estimation scheme

Therefore, a Lyapunov-based online parameter estimation procedure proposed in (Krstic, 2006) and successfully applied to other particle processes in (Dürr et al., 2015; Golovin et al., 2019) or to simulated granulation processes (Palis and Kienle, 2013, 2017) will be applied for the parameters a_i. In contrast to previous contributions, the parameter estimation is not only investigated theoretically but also applied to actual measurement data. Here, the estimation scheme, as depicted in Fig. 2, consists of a modified plant model running in parallel to the actual plant and a parameter estimator adapting unknown parameters in the parallel model.

3.1 Design of the parameter estimator

In order to derive a parameter estimator, the modified parallel model is designed as follows

$$\begin{aligned}\frac{\partial \hat{n}}{\partial t} =& -G\frac{\partial n}{\partial L} + \left(T_{\mathrm{sc1}}T_{\mathrm{sc2}} - T_{\mathrm{sc2}}T_{\mathrm{sc1}}\right) T_{\mathrm{out}} K n \\ &+ \left(\sum_{i=1}^{N-1} \hat{a}_i \phi_i(L) + \bar{\varphi}_i(L)\right) \int_0^\infty L^3 \dot{n}_{\mathrm{over}}\,\mathrm{d}L \\ &- c(\hat{n} - n)\end{aligned} \tag{19}$$

where $\hat{n}$ and $\hat{a}_i$ are the estimates of the number density distribution n and the mill coefficients a_i respectively. The parameter c acts as an additional tuning parameter for the observer term. Accordingly, the estimation errors are defined as

$$e = \hat{n} - n \tag{20}$$

$$\tilde{a}_i = \hat{a}_i - a_i \tag{21}$$

Based on the process and parallel model, i.e. eq. (18) and (19), the error system dynamics are given as follows.

$$\frac{\partial e}{\partial t} = \left(\sum_{i=1}^{N-1} \tilde{a}_i \phi_i(L)\right) \int_0^\infty L^3 \dot{n}_{\mathrm{over}}\,\mathrm{d}L - ce \tag{22}$$

$$\dot{\tilde{a}}_i = \dot{\hat{a}}_i \tag{23}$$

To determine the unknown parameters a_i, update laws for $\hat{a}_i$ have to be found such that the error system described by equations (22) and (23) is asymptotically stable. Choosing the following positive definite candidate Lyapunov functional

$$V = \frac{1}{2}\int_0^\infty e^2\,\mathrm{d}L + \sum_{i=1}^{N-1} \frac{1}{2\gamma_i}\tilde{a}_i^2 \tag{24}$$

where γ_i are additional tuning parameters, the error system is stable if the time derivative of V along the system trajectories is negative definite.

$$\begin{aligned}\dot{V} &= \int_0^\infty e\dot{e}\,\mathrm{d}L + \sum_{i=1}^{N-1} \frac{1}{\gamma_i}\tilde{a}_i\dot{\hat{a}}_i \\ &= \int_0^\infty e\left(\sum_{i=1}^{N-1} \tilde{a}_i\phi_i(L)\int_0^\infty L^3\dot{n}_{\mathrm{over}}\,\mathrm{d}L - ce\right)\mathrm{d}L \\ &\quad + \sum_{i=1}^{N-1} \frac{1}{\gamma_i}\tilde{a}_i\dot{\hat{a}}_i\end{aligned} \tag{25}$$

Here, the following update laws for $\hat{a}_i$

$$\dot{\hat{a}}_i = -\gamma_i \int_0^\infty e\phi_i(L)\,\mathrm{d}L \int_0^\infty L^3\dot{n}_{\mathrm{over}}\,\mathrm{d}L \tag{26}$$

result in a negative semi-definite time derivative of the Lyapunov functional

$$\dot{V} = -c\int_0^\infty e^2\,\mathrm{d}L \leq 0, \tag{27}$$

proving stability. However, for convergence of the parameter estimation errors towards zero, asymptotic stability has to be shown. According to LaSalle's invariance principle (Khalil, 2015) the error system converges towards the smallest invariant subset M_I of the set $M = \{(e, \tilde{a}_1, \ldots, \tilde{a}_{N-1}) \mid \dot{V} = 0\}$. For $e = 0$ and the linear independence of Gaussian functions with different mean values from equation (22) follows that $\frac{\partial e}{\partial t} = 0$ only holds if $\tilde{a}_i = 0$ for all i. Hence, $M_I = \{(0, 0, \ldots, 0)\}$ is the smallest subset invariant of the error system dynamics, resulting in asymptotic convergence of the parameter estimation errors towards zero.

Compared to other parameter estimation strategies, the theoretical proof of convergence even for the nonlinear process model is besides its simplicity a major advantage of the presented scheme. For a practical implementation of the update scheme the estimates $\hat{a}_i$ are restricted to positive values. The measurement of the particle size distribution n has been performed using an inline probe (*IPP 70-s, Parsum GmbH Chemnitz, Germany*). Due to the considerable noise corruption of the measurement signals, the convergence rate has to be restricted, which was ensured by choosing the tuning parameters c and γ_i appropriately.Generally, the influence of noise on the parameter estimation still has to be investigated.

3.2 Simulation

The parameter estimation scheme depicted in Fig. 2 has been implemented in Matlab, where the population balance model has been discretized along the property coordinate using the finite volume method (first-order upwind scheme with 200 equidistand grid points). The mill function is modeled as the sum of three weighted Gaussian functions (Neugebauer et al., 2016).

$$\varphi(L) = \sum_{i=1}^{3} a_i\varphi_i(L) = \sum_{i=1}^{3} a_i \exp\left(\frac{(L-\mu_i)^2}{\sigma_i^2}\right) \tag{28}$$

The process and mill parameters used for simulation are presented in Table 1 and 2 respectively.

Table 1: Process parameters

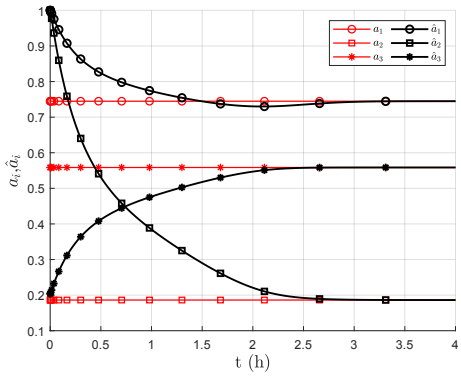

Fig. 3. Convergence of the unknown parameters $\hat{a}_i$ (black) to the actual parameters a_i (red)

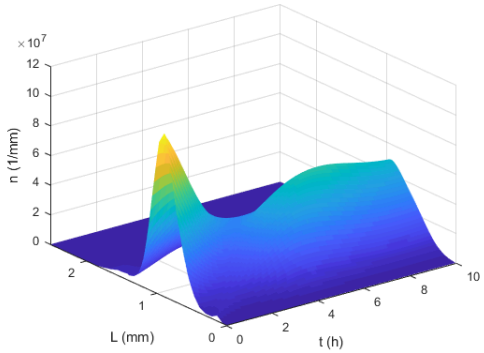

Fig. 4. PSD of the simulated process

Par.	Value	Par.	Value
$\dot{m}_{\text{inj}}$	0.0336 g s^{-1}	ρ	0.014 g mm^{-3}
L_{sc1}	1.18 mm	σ_{sc1}	0.055 mm
L_{sc2}	0.8 mm	σ_{sc2}	0.065 mm
		σ_{out}	0.5 mm

Table 2: Parameters of the mill

Par.	Value	Par.	Value	Par.	Value
a_1	0.745	μ_1	0.5 mm	σ_1	0.2 mm
a_2	0.186	μ_2	0.8 mm	σ_2	0.1 mm
a_3	0.559	μ_3	1.1 mm	σ_3	0.1 mm

As can be seen in Fig. 3, all three parameter estimates converge within roughly 3h, which is reasonable for the slow process behavior depicted in Fig. 4. In addition, as is shown in Fig. 5, the normalized L_2-norm of e also converges to zero in the same time frame.

3.3 Experimental validation

In this section the parameter estimation algorithm is applied to real process measurement presented in Neugebauer et al. (Neugebauer et al., 2019), covering $T = 19.7h$ with a sampling rate of 20 minutes. For the mill model 20 weighted Gaussian normal distributions with equal standard deviation σ_i and equidistant mean value

$$\mu_i = 0.1 + 0.1i \quad \text{for} \quad i = 1, \ldots, 20. \tag{29}$$

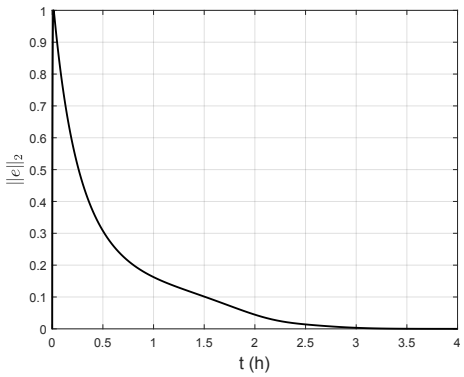

Fig. 5. Convergence of the normalized error L_2-norm

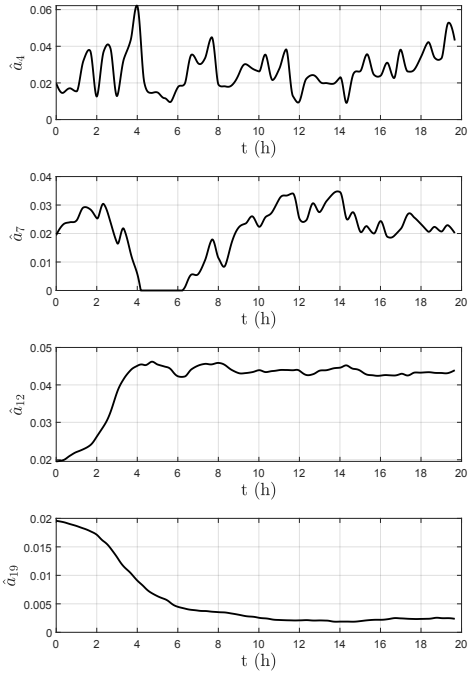

Fig. 6. Temporal evolution of the parameter estimates $\hat{a}_i$

turned out to be a suitable number of ansatz functions considering compuational effort and accuracy of the results. The initial parameter guesses and tuning parameters are given in Tab. 3. The tuning parameters were determined iteratively and are chosen, such that convergence speed of the estimator is reasonably fast without being too sensitive to measurement and process noise.

Table 3: Parameters parameter estimation

Par.	Value	Par.	Value
$\hat{a}_i(0)$	0.0171	σ_i	0.05
γ_i	10^{-14}	c	0.03

The adaption of the parameter estimates over time is depicted in Fig. 6 for 4 selected parameters. As can been seen, measurement noise and inner process variations do have a significant influence on the convergence behavior,

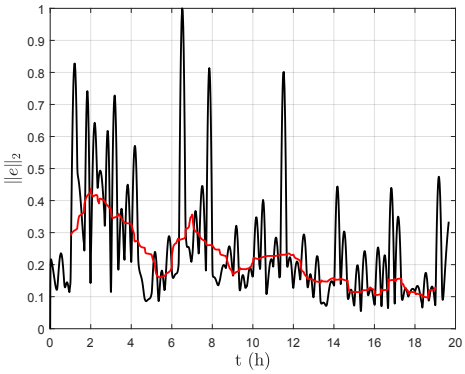

Fig. 7. Normalized L_2-norm of the plant-model-error e real (black) and averaged (red)

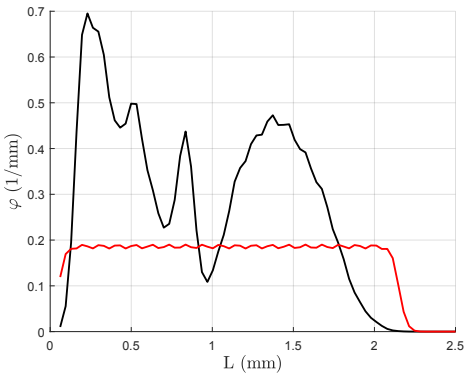

Fig. 8. Identified (black) and initial (red) mill function

especially for parameters connected to small particles size classes, exemplified by parameter estimate $\hat{a}_4$. In contrast to this, parameter estimate $\hat{a}_{19}$, which is connected to bigger particle size classes, clearly converges. The bigger influence of process noise on smaller particles can be an explanation for this phenomenon. The influence of noise is also clearly visible in the L_2-norm of the error depicted in Fig. 7. Nevertheless, the mill function identified for the final time point shown in Fig. 8 looks reasonable.

In order to further validate the parameter estimates, simulation results of a model using the identified mill function have been compared to the measurement data. Fig. 9 shows the respective particle size distributions over time. Both graphs suggest that the process will reach a stable equilibrium distribution. To validate the quality of the simulated plant model, the L_2-norm of PSD difference

$$e_{\mathrm{val}}(L,t) = n_{\mathrm{meas}}(L,t) - n_{\mathrm{sim}}(L,t) \tag{30}$$

is computed for every time step. Furthermore, it is compared to a simulation using initial guesses for the mill parameters. As shown in figure 10 the error L_2-norm decreases over time, which indicates good model-plant agreement near the steady state. Furthermore, the difference between simulated and measured plant is nearly always smaller compared to the simulation using the initial parameter guesses. For a more convenient representation, the respective PSDs are presented at four selected time instants in Fig. 11. While the simulation and measurement differ noticeably during the transitional phase, there is

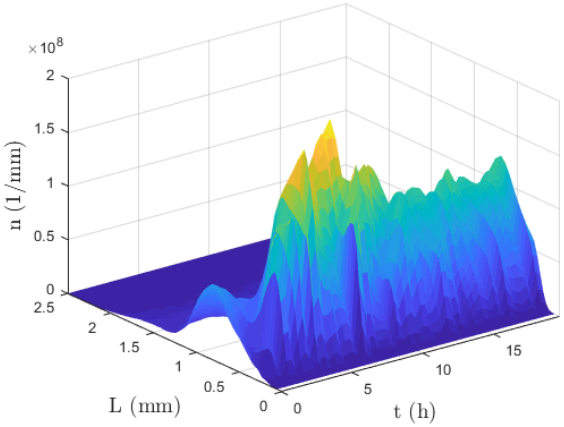

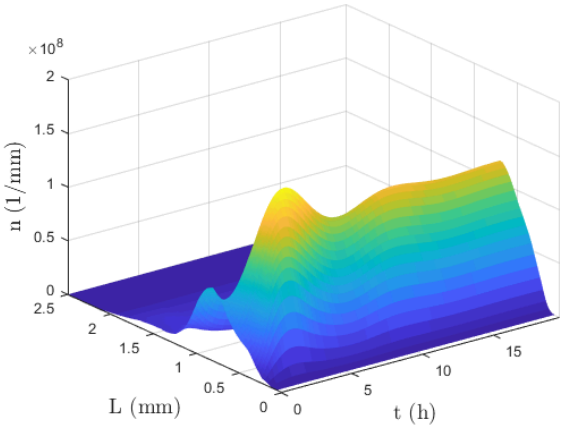

Fig. 9. Measured (top) and simulated (bottom) particle size distributions $n_{\mathrm{meas}}(L,t)$ and $n_{\mathrm{sim}}(L,t)$

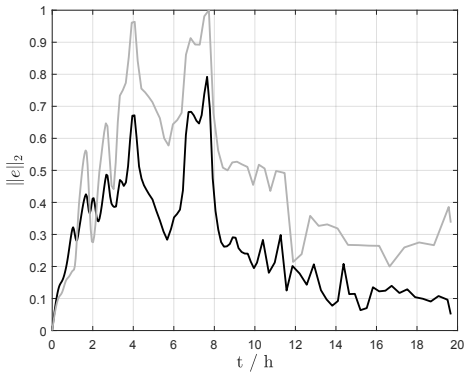

Fig. 10. Normalized L_2-norm of the validation error $e_{val}(L,t)$ with identified mill parameters (black) and using initial guesses (grey)

nearly perfect agreement between plant and simulation at $t \approx 20$h.

4. CONCLUSION AND OUTLOOK

In this contribution a Lyapunov-based online parameter estimation scheme for identifying mill function parameters in a fluidized bed layering granulation process was derived and tested in a simulation environment and with real mea-

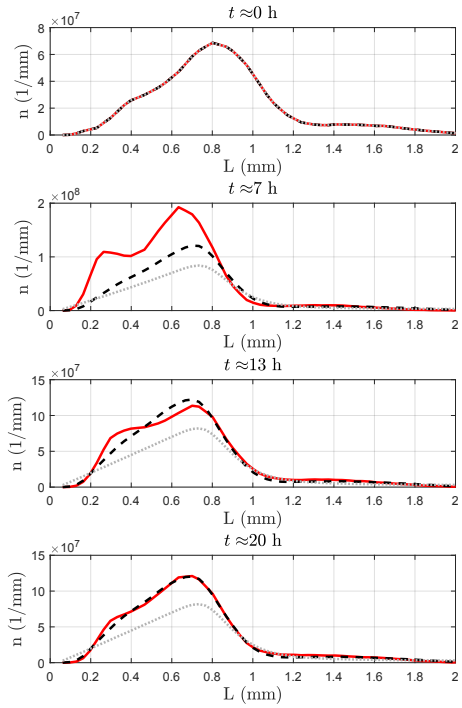

Fig. 11. Particle size distributions n(L,t) measured (red), simulated with estimated parameters (black, dotted) and simulated with parameter initial guesses (grey, dashed)

surement data. In the first case the parameter estimates converge towards the desired values as the theoretical derivation predicts. In the case of the measured data the convergence of the parameters is not as obvious due to measurement noise and inner process variations. To verify the quality of the identification, the plant was simulated using the identified mill function and then compared to the measurements.

In future contributions the estimation scheme can be used to identify time varying mill models capturing the non-steady state dynamics of the process. Furthermore, the proposed parameter estimation method can be used as a basis for an adaptive controller design.

ACKNOWLEDGEMENTS

The financial support of DFG (Deutsche Forschungsgemeinschaft) within the priority program SPP 1679 is gratefully acknowledged.

REFERENCES

Dreyschultze, C., Neugebauer, C., Palis, S., Bück, A., Tsotsas, E., Heinrich, S., and Kienle, A. (2015). Influence of zone formation on stability of continuous fluidized bed layering granulation with external product classification. *Particuology*, 23, 1 – 7.

Dürr, R., Palis, S., and Kienle, A. (2015). Online parameter identification of facet growth kinetics in crystal morphology population balance models. *Procedia Engineering*, 102, 1336 – 1345. New Paradigm of Particle Science and Technology Proceedings of The 7th World Congress on Particle Technology.

Golovin, I., Otto, E., Dürr, R., Palis, S., and Kienle, A. (2019). Lyapunov-based online parameter estimation in continuous fluidized bed spray agglomeration processes. *IFAC-PapersOnLine*, 52(1). 12th IFAC Symposium on Dynamics and Control of Process Systems, including Biosystems DYCOPS 2019.

Heinrich, S., Peglow, M., Ihlow, M., Henneberg, M., and Mörl, L. (2002). Analysis of the start-up process in continuous fluidized bed spray granulation by population balance modelling. *Chemical Engineering Science*, 57(20), 4369 – 4390. Particulate Processes.

Khalil, H.K. (2015). *Nonlinear Control*. Pearson.

Krstic, M. (2006). Systematization of approaches to adaptive boundary stabilization of PDEs. *International Journal of Robust and Nonlinear Control*, 16(16), 801–818.

Mörl, L., Heinrich, S., and Peglow, M. (2007). Chapter 2 fluidized bed spray granulation. In A. Salman, M. Hounslow, and J. Seville (eds.), *Granulation*, volume 11 of *Handbook of Powder Technology*, 21 – 188. Elsevier Science B.V.

Neugebauer, C., Diez, E., Bück, A., Palis, S., Heinrich, S., and Kienle, A. (2019). On the dynamics and control of continuous fluidized bed layering granulation with screen-mill-cycle. *Powder Technology*, 354, 266–277.

Neugebauer, C., Palis, S., Bück, A., Diez, E., Heinrich, S., Tsotsas, E., and Kienle, A. (2016). Influence of mill characteristics on stability of continuous layering granulation with external product classification. volume 38 of *Computer Aided Chemical Engineering*, 1275–1280. Elsevier.

Palis, S. and Kienle, A. (2013). Online parameter identification for continuous fluidized bed spray granulation. In *5th International Conference on Population Balance Modelling (PBM)*.

Palis, S. and Kienle, A. (2017). Online parameter identification for continuous fluidized bed spray granulation with external sieve-mill cycle. In *2017 22nd International Conference on Methods and Models in Automation and Robotics (MMAR)*, 594–598.

Palis, S. and Kienle, A. (2012). Stabilization of continuous fluidized bed spray granulation with external product classification. *Chemical Engineering Science*, 70, 200 – 209. 4th International Conference on Population Balance Modeling.

Palis, S. and Kienle, A. (2014). Discrepancy based control of particulate processes. *Journal of Process Control*, 24(3), 33 – 46.

Radichkov, R., Müller, T., Kienle, A., Heinrich, S., Peglow, M., and Mörl, L. (2006). A numerical bifurcation analysis of continuous fluidized bed spray granulation with external product classification. *Chemical Engineering and Processing: Process Intensification*, 45(10), 826 – 837.

Schmidt, M., Rieck, C., Bück, A., and Tsotsas, E. (2015). Experimental investigation of process stability of continuous spray fluidized bed layering with external product separation. *Chemical Engineering Science*, 137, 466 – 475.